

# Preserved flora and organics in impact melt breccias

P.H. Schultz<sup>1\*</sup>, R. Scott Harris<sup>2</sup>, S.J. Clemett<sup>3</sup>, K.L. Thomas-Keptra<sup>3</sup>, and M. Zárate<sup>4</sup>

<sup>1</sup>Department of Geological Sciences, Brown University, Providence, Rhode Island 02912, USA

<sup>2</sup>Office of Materials and Testing, Georgia Department of Transportation, Forest Park, Georgia 30297, USA

<sup>3</sup>Jacobs Technology Inc., 2224 Bay Area Boulevard, Houston, Texas 77058, USA

<sup>4</sup>CONICET/FCEN–Universidad Nacional de la Pampa, Avenida Uruguay 151, 6300 Santa Rosa, La Pampa, Argentina

## ABSTRACT

Impact cratering can destroy life from local to global scales and result in sudden turnovers of dominant genera and/or species. Here we report that it can also preserve components of the local biology present at the time of impact. We have investigated floral matter encapsulated within Cenozoic Era impact glasses produced by separate bolide impacts into the loessoid sediments of Argentina that occurred between 9.2 Ma (Miocene) and 6 ka (Holocene). The encapsulation preserved not only macro-scale morphological biosignatures such as vascular bundles, veins, phytoliths, and papillae, but also structures down to the cellular level. In the best-preserved samples we also found evidence for organic matter. While fossilization typically occurs over an extended time period as minerals slowly replace organic matter and the host rock lithifies under pressure, the process documented here is instantaneous. Preservation of morphological and chemical biosignatures in impact events can provide snapshots of the ecology in environments that do not otherwise promote a diverse fossil record. We suggest that this would provide a new strategy for identifying signs of possible early life on ancient Mars, where similar target conditions once existed.

## INTRODUCTION

At least seven glass-bearing layers of varying ages dating back to the Miocene occur at different horizons in the Pampean strata of Argentina (Schultz et al., 1994, 1998, 2004). Because they predate human occupation, their origin presented an enigma in the early 20<sup>th</sup> century; however, there is now compelling evidence that they formed through bolide impacts. The glasses have specific radiometric ages that are consistent with regional biostratigraphic, magnetostratigraphic, and lithostratigraphic frameworks (Schultz et al., 2004, 2006), and in several cases are coincident with the disappearance of endemic fauna (Schultz et al., 1998, 2006; Vizcaíno et al., 2004). The formation process involved rapid thermal excursions, quenching, and shock metamorphism, as evidenced by (1) planar deformation features (PDFs) in quartz and other silicates; (2) thetamorphic phases (e.g., lechatelierite, diaplectic feldspar); (3) ultrahigh-temperature decomposition reactions (e.g., zircon → baddeleyite, chromite → eskolaite) and melting (e.g., rutile); and (4) quench textures (see Schultz et al., 2004, 2006; Harris and Schultz, 2005, 2007; Harris et al., 2005a, 2005b).

In a strict sense, these impact glasses are melt-matrix breccias with glass containing loessoid sediments, partially digested mineral clasts, and basement fragments. <sup>40</sup>Ar/<sup>39</sup>Ar dating yielded ages ( $\pm 2\sigma$ ) of  $6 \pm 2$  ka,  $114 \pm 26$  ka,  $230 \pm 30$  ka,  $445 \pm 21$  ka,  $3.27 \pm 0.08$  Ma,  $5.28 \pm 0.04$  Ma, and  $9.21 \pm 0.08$  Ma (Schultz et al., 1998, 2004, 2006). Where found in place (see Fig. DR1 in the GSA Data Repository<sup>1</sup>), these ages are consistent with the local stratigraphy and faunal assemblages (Zárate, 2003). A striking property of some of these impact glasses (Fig. 1) is the encapsulation

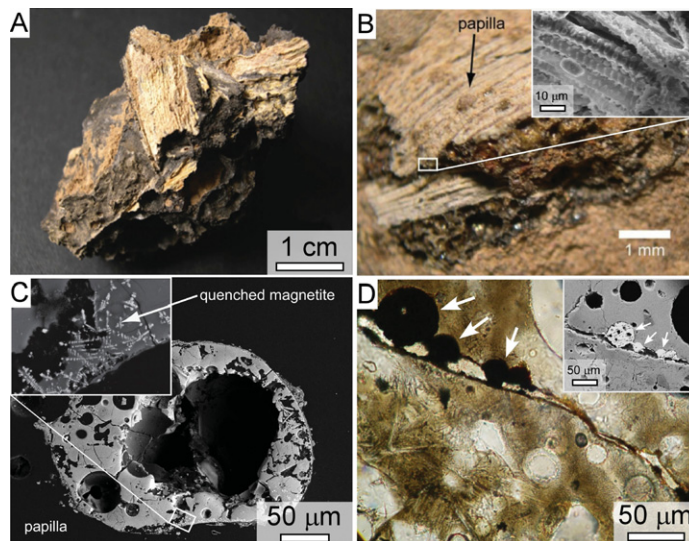


**Figure 1.** Optical and scanning electron microscope (SEM) images of Chasicó (CH), Argentina, impact-melt breccia samples. **A:** Macroscopic preservation of Miocene leaves. **B:** Close-up showing overlapping vitrified leaves with hemispherical papilla present on upper leaf surface (black arrow). Inset SEM image shows preservation of cellular features, including saddle-shaped silica bodies, cork cells, and stoma. **C:** Backscattered SEM image showing underside of large papillae in B. Vesiculation and dendritic magnetite crystals (inset) indicate that the leaf was heated to very high temperatures and then rapidly quenched. **D:** Polarized optical image of leaf cross section with inset backscattered SEM image. Distinctive black spherical features on upper leaf surface (white arrows) are composed of iron oxides resulting from bacterial activity.

of preserved fragments of floral and soft-tissue faunal remains (Harris and Schultz, 2007). Other studies have noted the presence of flora impressions but did not assess possible remains (Osinski et al., 2007).

Using impact glasses from the Chasicó (CH;  $9.21 \pm 0.08$  Ma) and Mar del Plata (MdP;  $3.27 \pm 0.08$  Ma) regions, we investigated the conditions necessary for encapsulation and preservation of plant matter. Three analytical methods were used: two-step laser desorption/laser ionization mass spectrometry ( $\mu$ -L<sup>2</sup>MS); field emission scanning electron microscopy (FESEM) with light element energy dispersive X-ray spectrometry (EDX); and transmission electron microscopy (TEM), as described in the Data Repository.

## ANALYTICAL RESULTS

### Optical and Scanning Electron Microscopy

Figures 1 and 2 show optical and SEM images of CH and MdP impact glasses containing encapsulated plant matter (Figs. DR2–DR4; Movies DR1–DR3). In the largest samples (Figs. 1A and 1B), centimeter-scale leaf fragments are recognizable and exhibit readily discernible macro-scale features such as veins, ribs, and papillae (Figs. 1C and 1D). Electron microprobe analyses of the surface of these materials closely match the composition of the impact glass and indicate rapid quenching (Fig. 1C). Opaque

\*E-mail: E-mail: peter\_schultz@brown.edu.

<sup>1</sup>GSA Data Repository item 2014183, further discussion of the impact origin of the glasses; methods; additional figures providing further context for locations, regions selected for analyses, and additional examples; and movies providing perspective of materials trapped in the glass, is available online at [www.geosociety.org/pubs/ft2014.htm](http://www.geosociety.org/pubs/ft2014.htm), or on request from [editing@geosociety.org](mailto:editing@geosociety.org) or Documents Secretary, GSA, P.O. Box 9140, Boulder, CO 80301, USA.

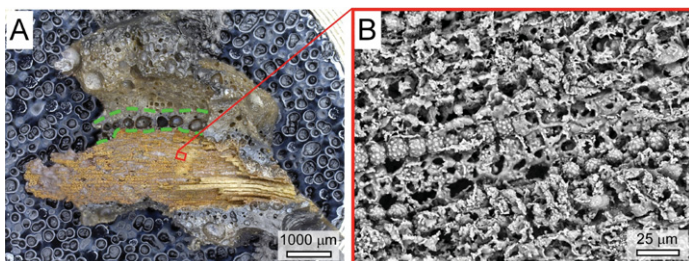


**Figure 2.** Optical and scanning electron microscope (SEM) images of freshly exposed leaf preserved in Mar del Plata (MdP), Argentina, impact glass. **A:** Optical image of sample on black C-tape, with orange leaf surrounded by darkened, vesiculated, frothy rim of glass (dashed green lines). **B:** Backscattered SEM image of region enclosed by red box in A, showing cellular-scale morphological preservation of structures, including papillae and phytoliths.

hemispherical growths (Fig. 1D) on some entrained leaf surfaces are iron oxide. Prominent twinning suggests that they are dehydrated iron hydroxides, which commonly form by bacterial precipitation on decaying vegetation (Dunn et al., 1997). Parallel-striated assemblages composed of vein-like features (Figs. 2 and 3) resemble vascular bundles found in tracheophytes such as pampas grass. At high magnifications, these striated assemblages become subparallel rows of phytoliths (Figs. 2A and 2B), with individual phytoliths resembling eroded stellated polyhedra (Fig. 3A). Intermingled among the phytoliths is a disorganized fibrous matter, interpreted as degraded cellular material in various states of preservation (Fig. 3B), and blade-shaped phyllosilicate bundles (Fig. 3C). EDX analyses of both the preserved cellular material and associated phyllosilicates demonstrate the presence of major (i.e.,  $\geq 1$  wt%) amounts of carbon (Figs. 3D and 3E).

### Transmission Electron Microscopy

TEM analysis of ultramicrotomed thin sections ( $\sim 200 \times 300 \mu\text{m}$  in area and  $\sim 100$  nm thick) of MdP and CH samples showed that they are

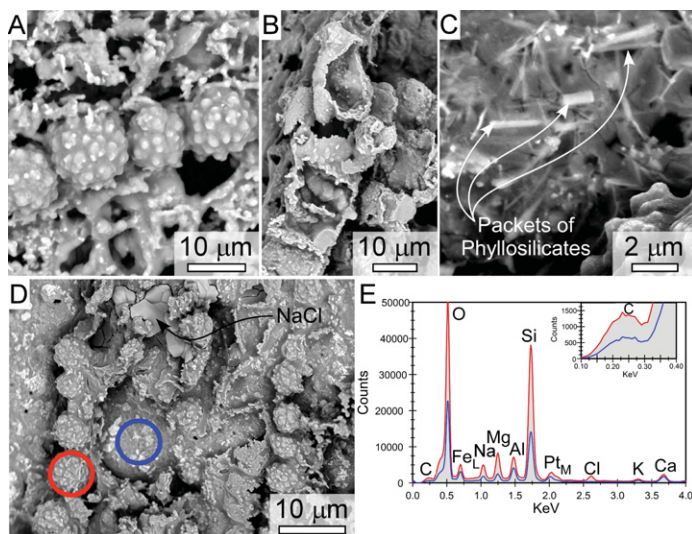


**Figure 3.** Scanning electron microscope (SEM) images and energy dispersive X-ray spectrometry (EDX) spectra of preserved leaf fragment from Figure 2. **A:** Linear chain of phytoliths showing distinctive stellated polyhedral morphology. **B:** Edge-on view of a sheet of cells in various states of degradation. **C:** Packets of phyllosilicates dispersed within leaf remnant. **D:** SEM image with red and blue circles indicating areas from which EDX spectra in E were taken. **E:** EDX spectra illustrating carbon enrichment associated with phytoliths and phyllosilicate packets (red circle in D) compared to background (blue circle in D).

composed of intermixed assemblages of four texturally and chemically distinct phases: (1) degraded plant matter; (2) impact glass; (3) phyllosilicate-rich bundles; and (4) crystalline mineral grains. The degraded plant matter (Fig. 4) appears structureless, and selected area electron diffraction indicated that it is amorphous. EDX point spectra revealed that the major elements present were C, O, Mg, Al, Si, and Fe (Figs. 4B and 4E), with the C abundance enriched  $\sim 4\times$  over that of the surrounding glass. The glass was composed of slender elongated grains ranging in length from  $\sim 0.1$  to  $1 \mu\text{m}$ ; the upper size limit is likely constrained by chattering during microtome cutting (Fig. 4). Bordering but clearly delineated from the glassy fragments were bundles of phyllosilicates (Figs. 4A and 4D), some of which were also embedded within the plant matter. Lattice spacings of  $\sim 1.0$ – $1.1$  nm are consistent with smectite-type clays (Fig. 4D). EDX spectra showed C, O, Mg, Al, Si, and Fe, with abundances similar to those expected for smectite, albeit with excess Si and major C (Figs. 4C and 4F). Crystalline grains, including silicates, Fe-oxides, and sulfates, as large as  $\sim 1 \mu\text{m}$ , were observed distributed throughout the previous three phases (Fig. 4A).

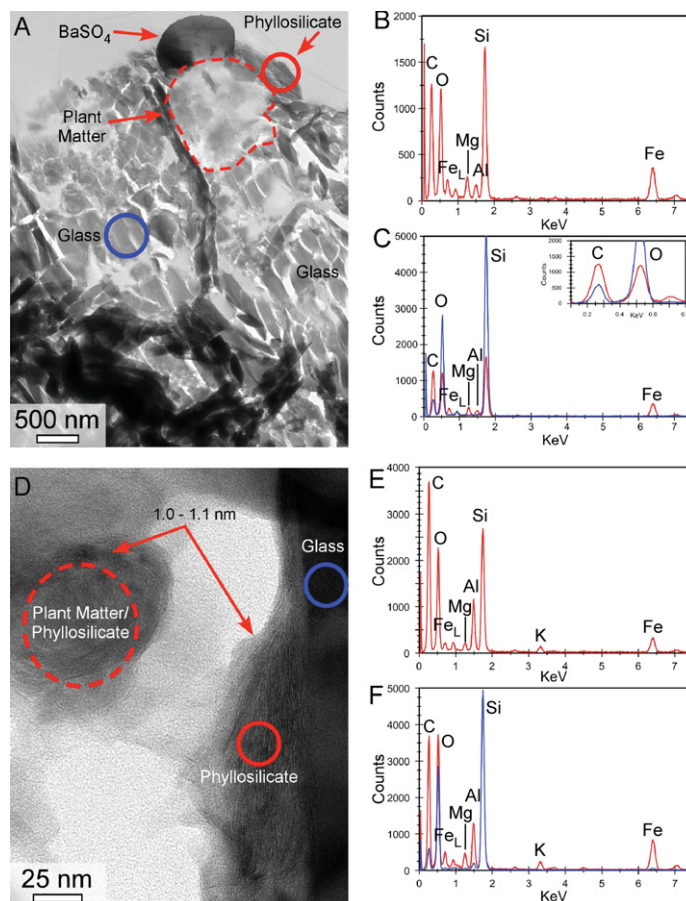


**Figure 4.** Transmission electron microscopy (TEM) images and associated energy dispersive X-ray spectrometry (EDX) spectra of preserved flora in Mar del Plata (MdP) and Chasicó (CH), Argentina, impact-melt breccias. **A:** TEM image of plant matter embedded within MdP melt glass, partially surrounded by phyllosilicates and abutting  $\text{BaSO}_4$  crystallite. **B:** EDX spectrum of plant matter (region in red dashed line in A) showing a high carbon abundance. **C:** EDX spectra of phyllosilicates (red spectrum; solid red circle in A) and glass (blue spectrum; blue circle in A) indicating that the phyllosilicates are also enriched in carbon. **D:** Leaf material preserved in CH impact glass with associated smectite-type phyllosilicates ( $1.0$ – $1.1$  nm basal spacings). **E:** EDX spectrum of leaf material (red dashed circle in D) illustrating the high carbon abundance. **F:** EDX spectra of phyllosilicates (red spectrum; red circle in D) and glass (blue spectrum; blue circle in D) showing carbon enrichment in the phyllosilicates but not in the glass.



## Two-Step Laser Mass Spectrometry Analysis

We used  $\mu$ -L<sup>2</sup>MS to investigate whether organic material was associated with preserved leaf fragments. Analyses were performed using both ultraviolet (UV) and vacuum ultraviolet (VUV) photoionization and a sample analysis spot resolution of  $\sim 7\ \mu\text{m}$ . UV photoionization is selective to the presence of aromatic and/or conjugated organic species (Clemett and Zare, 1996), whereas VUV photoionization provides a broad window for virtually all organic species (Shi and Lipson, 2005).

Figure 5 summarizes the results from the analysis of several Mar del Plata (MdP) samples (Figs. DR1 and DR2; Movie DR1). Figure 5A shows summed mass spectra acquired from embedded vascular material located  $\sim 100\ \mu\text{m}$  from the impact glass interface (see the analyzed region outlined in blue in Fig. DR2). The UV photoionization spectrum indicates a range of simple polycyclic aromatic hydrocarbons (PAHs) and their alkylated moieties; the most prominent are  $\text{C}_n$ -styrene [ $\text{C}_6\text{H}_5\text{CH}=\text{C}(\text{CH}_2)_n\text{H}$ ;  $n = 0, 1 \rightarrow 104, 118\ \text{amu}$ ],  $\text{C}_n$ -naphthalene [ $\text{C}_{10}\text{H}_8-(\text{CH}_2)_n\text{H}$ ;  $n = 0, 1, 2 \rightarrow 128, 142, 156\ \text{amu}$ ] and  $\text{C}_n$ -phenanthrene [ $\text{C}_{14}\text{H}_{10}-(\text{CH}_2)_n\text{H}$ ;  $n = 0, 1, 2 \rightarrow 178,$

192, 206 amu]. In addition, there was evidence for oxidized substituents in the form of hydroxy ( $-\text{OH}$ ) and methoxy ( $\text{CH}_3\text{O}-$ ) functional groups, e.g., phenol ( $\text{C}_6\text{H}_5\text{OH}$ ; 94 amu). The VUV photoionization spectrum indicates that the overall abundance of organic matter is dominated by short-chain ( $\text{C}_2$ - $\text{C}_6$ ) alkanes and alkenes.

Figure 5B shows summed mass spectra acquired from the vascular material located  $\sim 1000\ \mu\text{m}$  from the impact glass interface. The abundance of aromatic organics was observed to increase by more than an order of magnitude, with a prominent cluster of higher mass peaks (i.e.,  $>300\ \text{amu}$ ) at 306, 312, and 318 amu. The variance in diversity and abundance of organics at different distances from the impact glass interface suggest that the interior of encapsulated plant matter was heated to a low temperature and for a shorter period than that those closer to the nascent impact glass interface. While absolute identification of the high mass peaks is ongoing, several inferences are possible: (1) the species are aromatic; (2) the preponderance of lower odd mass peaks implies N-containing functional groups; (3) the main 312 amu peak has an exact mass of  $312.15 \pm 0.01\ \text{amu}$ , requiring  $\sim 20\ \text{H}$  atoms per molecule; and (4) the peak intensities indicate a particularly stable species. Given the nature of the samples, tetracyclic pyrrole and/or pyrroline structures are consistent with these observations. For example, the chlorin ( $\text{C}_{20}\text{H}_{16}\text{N}_4$ ; 312.14 amu) is the core macrocycle in chlorophyll and related photosensitive pigments in chloroplasts. Closely related to chlorin is corrin ( $\text{C}_{19}\text{H}_{22}\text{N}_4$ ; 312.14 amu), and corrinoid ring structures also occur naturally in biological systems.

## Experimental Simulations of Impact Entrapment

A sequence of heating experiments constrained the conditions necessary for preservation of plant matter in impact glass. In order to simulate a natural system, samples were prepared by adding small leaf clippings of Argentine pampas grass, both wetted and unwetted (but not desiccated), to pulverized Argentine impact glass. These were then flash heated for 10, 60, and 300 s in a vertical-tube furnace at temperatures from 1000 °C to 1700 °C. For each time and temperature, three sample runs were performed at successively lower  $\text{O}_2$  fugacities by (1) using an open Pt crucible; (2) using an open Pt crucible with a graphite rod; and (3) using a sealed graphite tube and then quenching in ambient air.

Temperature was determined as the critical variable. Below 1500 °C, the fused glass assemblages invariably contained carbonized leaf fragments, without preservation of micro-scale or macro-scale leaf morphology. Above 1500 °C, leaf morphology was preserved and the visual appearance of the fused glass assemblages bore a striking resemblance to the natural samples (Fig. DR5). Consequently, entrainment of flora material in CH and MdP samples must have occurred via interaction at high temperatures ( $>1500\ ^\circ\text{C}$ ) with a low-viscosity, but rapidly quenched, silica melt. The survival of organic matter under these conditions requires (1) short-enough duration of the thermal excursion (i.e., seconds) to prevent thermodynamic equilibrium; and (2) local peak temperatures buffered by energy sinks such as the endothermic phase transitions (Bonny et al., 1988), dynamic pyrometamorphism of mineral phases (Rietmeijer, 2004), and the dehydration of hydrated silicates (Flynn, 1995).

## DISCUSSION

Three scenarios could account for the presence of plant material embedded within impact glasses studied here: (1) post-impact ingrowths and weathering; (2) flash melting of flora-rich surface sediments by an air burst; and (3) interactions with impact melt entrained in the cratering flow field or low-speed ballistic melts into water-rich sediments containing buried and/or decaying plant materials.

The first scenario can be discounted by our observations: (1) darkened, highly vesiculated, frothy rims around entrapped plant matter (Fig. 2A), indicative of still molten or semimolten glass during encapsulation; (2) sharp contact boundaries between glass and smectite-type phyllosilicates, which would have been lost during weathering; (3) the presence

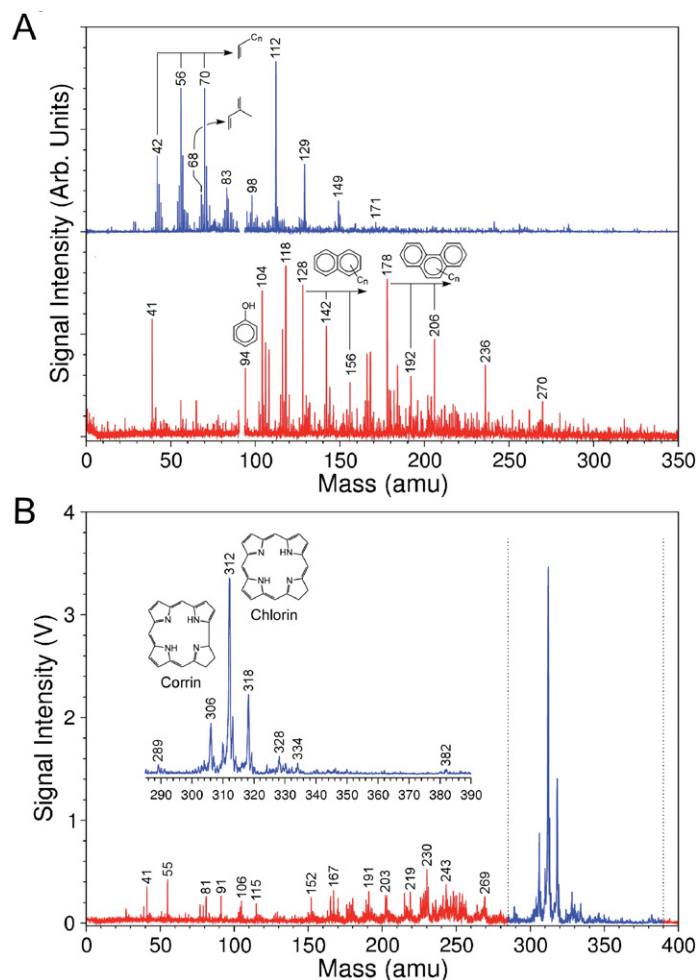


**Figure 5.** Mass spectra of preserved leaf fragment in Mar del Plata (MdP), Argentina, impact glasses (photo documentation in Figs. DR2 and DR3 [see footnote 1]). Arb.—arbitrary. **A:** Two-step laser desorption/ionization mass spectrometry ( $\mu$ -L<sup>2</sup>MS) mass spectra acquired using vacuum ultraviolet (VUV) (118 nm, blue) and UV (266 nm, red) photoionization of leaf material in close proximity ( $\sim 100\ \mu\text{m}$ ) to the impact glass interface. **B:**  $\mu$ -L<sup>2</sup>MS mass spectra acquired using UV photoionization of leaf material located at distance ( $>1000\ \mu\text{m}$ ) from the impact glass interface. Upper range of the mass spectrum in blue shows a prominent cluster of high mass peaks. The averaged spectra from multiple regions are shown at higher resolution in the inset spectrum. In both A and B, prominent mass peaks are indicated along with representative structures where relevant.

of phyllosilicates enriched in carbon compared to the surrounding glass, indicating that the latter phase was not the progenitor of the former; and (4) quench textures within vitrified papilla indicative of flash heating followed by rapid cooling (Figs. 1C and 1D).

The second scenario necessitates the instantaneous melting of surface sediments. This can also be discounted due to the presence of mixed clastic materials from depth and highly shocked minerals within the glasses (Schultz et al., 2004, 2006).

The third scenario is most consistent with our sample analyses and the observed cratering dynamics, including evidence for dynamic modes of ejection and emplacement with distorted vesicles and sediments trapped in seams (Schultz et al., 2004, 2006). It accounts for the presence of both shocked and unshocked mineral phases in close proximity to one another within the glasses. It also would explain the spatial association of plant matter and phyllosilicates. Both are enriched in C and Si, thereby requiring that the phyllosilicates were likely synthesized from amorphous silica (Motomura et al., 2000) present with the plant matter during post-shock cooling. As the impact melt came into contact with the water-rich sediment and plant detritus (whether during ejection or emplacement), it would be quenched by the endothermic phase transition of water turning to steam (i.e., >1500 K; Furukawa et al., 2011), which would then become trapped in vesicles within the cooling glassy matrix. As the temperature decreased, steam would condense out as water vapor that could subsequently interact with trapped plant matter to form smectite-type phyllosilicates. This process is analogous to the hydrothermal synthesis of smectites from amorphous gels (Kloprogge et al., 1999). Previous work has shown that synthetic smectite-type phyllosilicates can be prepared from gels composed of a variety of organic compounds such as porphyrins and organic dyes (Carrado et al., 1991, 1997).

## CONCLUSIONS AND IMPLICATIONS

Flora matter embedded in Argentine MdP and CH impact glasses provide the first examples of the preservation of biological material by impact cratering processes. The survival and preservation of organic matter within rapidly quenched impact glasses may provide a new strategy for identifying biomarkers of possible early life on Mars (Cockell et al., 2003). Specifically, thick air-fall sediments cover broad areas on Mars and should have trapped impact melt over billions of years under conditions conducive for preservation until exhumed (Schultz and Mustard, 2004).

## ACKNOWLEDGMENTS

We gratefully acknowledge partial support through NASA grants NAG5-12327 and NNX13AB75G (Schultz) and the Rhode Island Space Grant Program (Harris). We thank O. Clemett, C. Clemett, S. Keprta, and N. Keprta for their assistance. We also thank three anonymous reviewers for their constructive comments.

## REFERENCES CITED

Bonny, P., Balageas, D., Devezeaux, D., and Maurette, M., 1988, Atmospheric entry of micrometeorites containing organic materials: 19<sup>th</sup> Lunar and Planetary Science Conference extended abstracts, p. 118–119.

Carrado, K.A., Thiagarajan, R.E., Winas, R.E., and Botto, R.E., 1991, Hydrothermal crystallization of porphyrin-containing layer silicates: *Inorganic Chemistry*, v. 30, p. 794–799, doi:10.1021/ic00004a034.

Carrado, K.A., Thiagarajan, P., and Song, K., 1997, A study of organo-hectorite clay crystallization: *Clay Minerals*, v. 32, p. 29–40, doi:10.1180/claymin.1997.032.1.05.

Clemett, S.J., and Zare, R.N., 1996, Microprobe two-step laser mass spectrometry as an analytical tool for meteoritic samples, in van Dishoeck, E.F., ed., *Molecules in astrophysics: Probes and processes*: International Astronomical Union (IAU) Symposium 178: Leiden, Netherlands, Springer, p. 305–320.

Cockell, C.S., Osinski, G.R., and Lee, P., 2003, The impact crater as a habitat: Effects of impact processing of target materials: *Astrobiology*, v. 3, p. 181–191, doi:10.1089/153110703321632507.

Dunn, K.A., McLean, R.J.C., Upchurch, G.R., Jr., and Folk, R.L., 1997, Enhancement of leaf fossilization potential by bacterial films: *Geology*, v. 25, p. 1119–1122, doi:10.1130/0091-7613(1997)025<1119:EOLFPB>2.3.CO;2.

Flynn, G.J., 1995, Thermal gradients in interplanetary dust particles: The effect of an endothermic phase transition: 26<sup>th</sup> Lunar and Planetary Science Conference extended abstracts, p. 405–406.

Furukawa, Y., Sekine, T., Kakegawa, T., and Nakazawa, H., 2011, Impact-induced phyllosilicate formation from olivine and water: *Geochimica et Cosmochimica Acta*, v. 75, p. 6461–6472, doi:10.1016/j.gca.2011.08.029.

Harris, R.S., and Schultz, P.H., 2005, Petrographic signatures of impacts into fine-grained porous sedimentary targets, in Evans, K.R., et al., eds., *The sedimentary record of meteorite impacts: SEPM (Society for Sedimentary Geology) Research Conference, Abstracts with Program*, p. 19.

Harris, R.S., and Schultz, P.H., 2007, Impact amber, popcorn, and pathology: The biology of impact melt breccias and implications for astrobiology: 38<sup>th</sup> Lunar and Planetary Science Conference, extended abstract no. 2306.

Harris, R.S., Schultz, P.H., and Bunch, T.E., 2005a, Accessory phases in Argentine impact breccias: Implications for shock history, emplacement dynamics, vapor composition and target lithologies: 36<sup>th</sup> Annual Lunar and Planetary Science Conference, extended abstract no. 1952.

Harris, R.S., Schultz, P.H., and Bunch, T.E., 2005b, Evidence for shocked feldspars and ballen quartz in 450,000 year old Argentine impact melt breccias: 36<sup>th</sup> Annual Lunar and Planetary Science Conference, extended abstract no. 1966.

Kloprogge, J.T., Komarneni, S., and Amonette, J.E., 1999, Synthesis of smectite clay minerals: A critical review: *Clays and Clay Minerals*, v. 47, p. 529–554, doi:10.1346/CCMN.1999.0470501.

Motomura, H., Fuji, T., and Suzuki, M., 2000, Distribution of silicified cells in the leaf blades of *Plieblastus chino* (Franchet et Savatier) Makino (Bambusoideae): *Annals of Botany*, v. 85, p. 751–757, doi:10.1006/anbo.2000.1124.

Osinski, G.R., Schwarcz, H.P., Smith, J.R., Kleindienst, M.R., Haldemann, A.F.C., and Churcher, C.S., 2007, Evidence for a ~200–100 ka meteorite impact in the Western Desert of Egypt: *Earth and Planetary Science Letters*, v. 253, p. 378–388, doi:10.1016/j.epsl.2006.10.039.

Rietmeijer, F.J.M., 2004, Dynamic pyrometamorphism during atmospheric entry of large (~10 micron) pyrrhotite fragments from cluster IDPs: *Meteoritics & Planetary Science*, v. 39, p. 1869–1887, doi:10.1111/j.1945-5100.2004.tb00082.x.

Schultz, P.H., and Mustard, J., 2004, Impact melts and glasses on Mars: *Journal of Geophysical Research*, v. 109, E01001, doi:10.1029/2002JE002025.

Schultz, P.H., Koeberl, C., Bunch, T., Grant, J., and Collins, W., 1994, Ground truth for oblique impact processes: New insight from the Rio Cuarto, Argentina, crater field: *Geology*, v. 22, p. 889–892, doi:10.1130/0091-7613(1994)022<0889:GTFIOIP>2.3.CO;2.

Schultz, P.H., Zárate, M., Hames, M., Camilion, C., and King, J.A., 1998, A 3.3-Ma impact in Argentina and possible consequences: *Science*, v. 282, p. 2061–2063, doi:10.1126/science.282.5396.2061.

Schultz, P.H., Zárate, M., Hames, B., Koeberl, C., Bunch, T., Storzer, D., Renne, P., and Wittke, J., 2004, The Quaternary impact record from the Pampas, Argentina: *Earth and Planetary Science Letters*, v. 219, p. 221–238, doi:10.1016/S0012-821X(04)00010-X.

Schultz, P.H., Zárate, M., Hames, W.E., Harris, R.S., Bunch, T.E., Koeberl, C., Renne, P., and Wittke, J., 2006, The record of Miocene impacts in the Argentine Pampas: *Meteoritics & Planetary Science*, v. 41, p. 749–771, doi:10.1111/j.1945-5100.2006.tb00990.x.

Shi, Y.J., and Lipson, R.H., 2005, An overview of organic molecule soft ionization using vacuum ultraviolet laser radiation: *Canadian Journal of Chemistry*, v. 83, p. 1891–1902, doi:10.1139/v05-193.

Vizcaíno, S.F., Fariña, R.A., Zárate, M.A., Bargo, M.S. and Schultz, P., 2004, Palaeoecological implications of the Mid-Pliocene faunal turnover in the Pampean Region (Argentina): *Palaeogeography, Palaeoclimatology, Palaeoecology*, v. 213, p. 101–113.

Zárate, M., 2003, The loess record of southern South America: *Quaternary Science Reviews*, v. 22, p. 1987–2006, doi:10.1016/S0277-3791(03)00165-3.

Manuscript received 2 December 2013

Revised manuscript received 17 March 2014

Manuscript accepted 17 March 2014

Printed in USA